Supplemental data

Myosin-X promotes breast cancer invasion and metastasis downstream of mutant p53

Antti Arjonen, Riina Kaukonen et al.

Inventory of supplemental data:

Supplemental data (Figures and figure legends)

Supplemental experimental procedures

Supplementary Figure 1

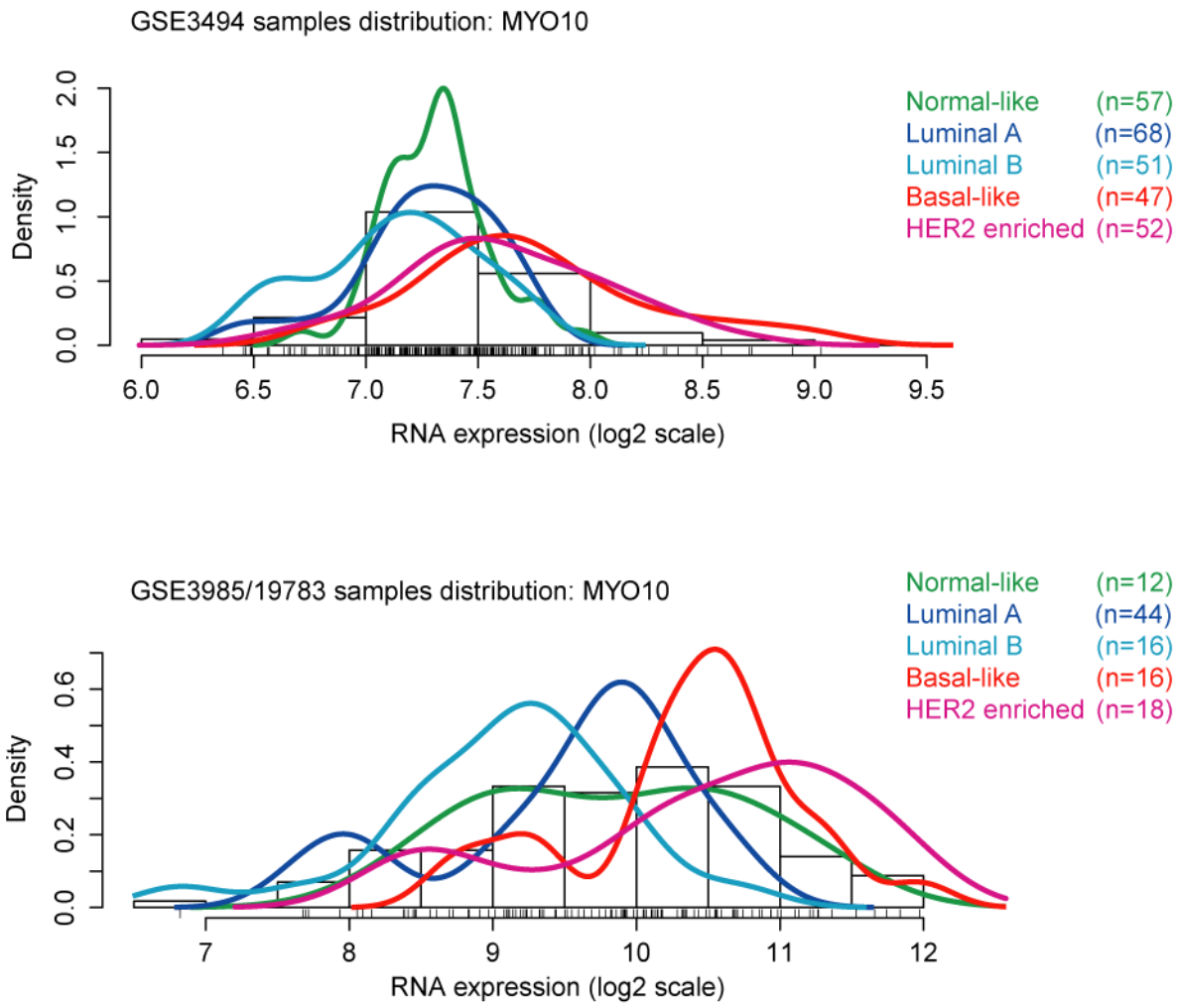

Figure S1

Myo10 expression is high in breast cancer subtypes with poor prognosis. The distribution of Myo10 mRNA expression in two independent datasets is shown. Total of 251 breast tumors (GSE3494; (Miller et al. 2005) and 104 breast tumors (GSE3985/19783; (Naume et al. 2007) and Myo10 mRNA levels are shown. Different colors indicate the clinical classification of the tumor and (*n*) the number of patients.

Supplementary Figure 2

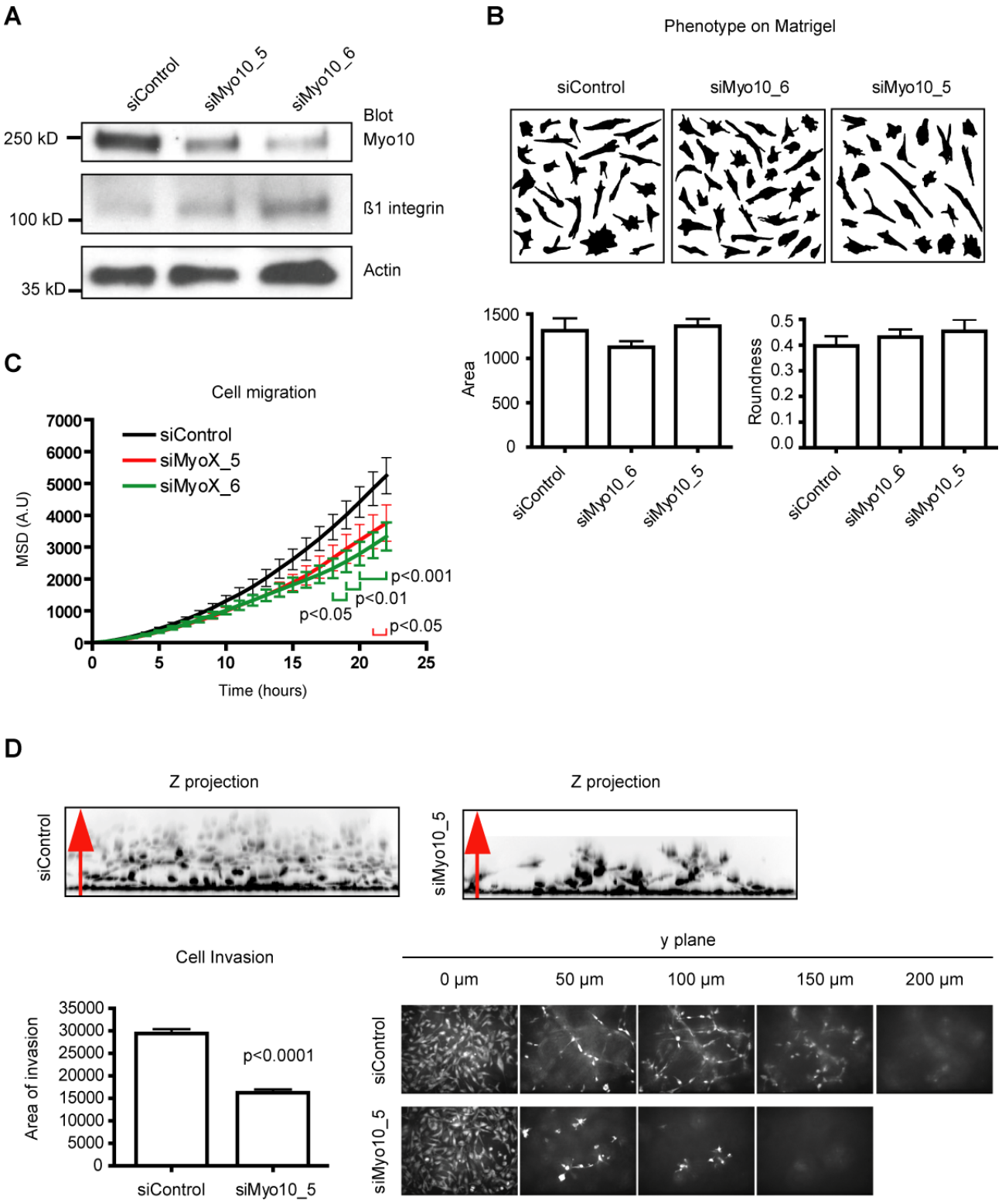

Figure S2

Silencing of Myo10 inhibits migration and invasion of breast cancer cells in vitro. (**A**) Western blot of Myo10 and β1-integrin levels in MDA-MB-231 cells transfected with the indicated siRNAs. Actin was blotted for loading control. (**B**) Morphology of siRNA-transfected MDA-MB-231 cells on Matrigel. Shown are cell outlines and calculated cell area and roundness (n = 23 to 37 cells). (**C**) Random migration of siRNA-transfected MDA-MB-231 cells on Matrigel. Cumulative mean square displacement of tracked cells is shown. n(siControl) = 43 and n(siMyo10_5 and siMyo10_6) = 25. (**D**) Invasion of the siRNA-transfected and Syto60 (cell body and nuclei)–stained MDA-MB-231 cell into Matrigel. Images show side views of invasion. Columns show invasion areas. The direction of invasion is indicated with a red arrow. The individual planes with the invaded cells and the invasion distance (from the bottom of the well) are shown (y-plane). Mean±SEM and Mann Whitney test are shown for all figures unless otherwise indicated.

Supplementary Figure 3

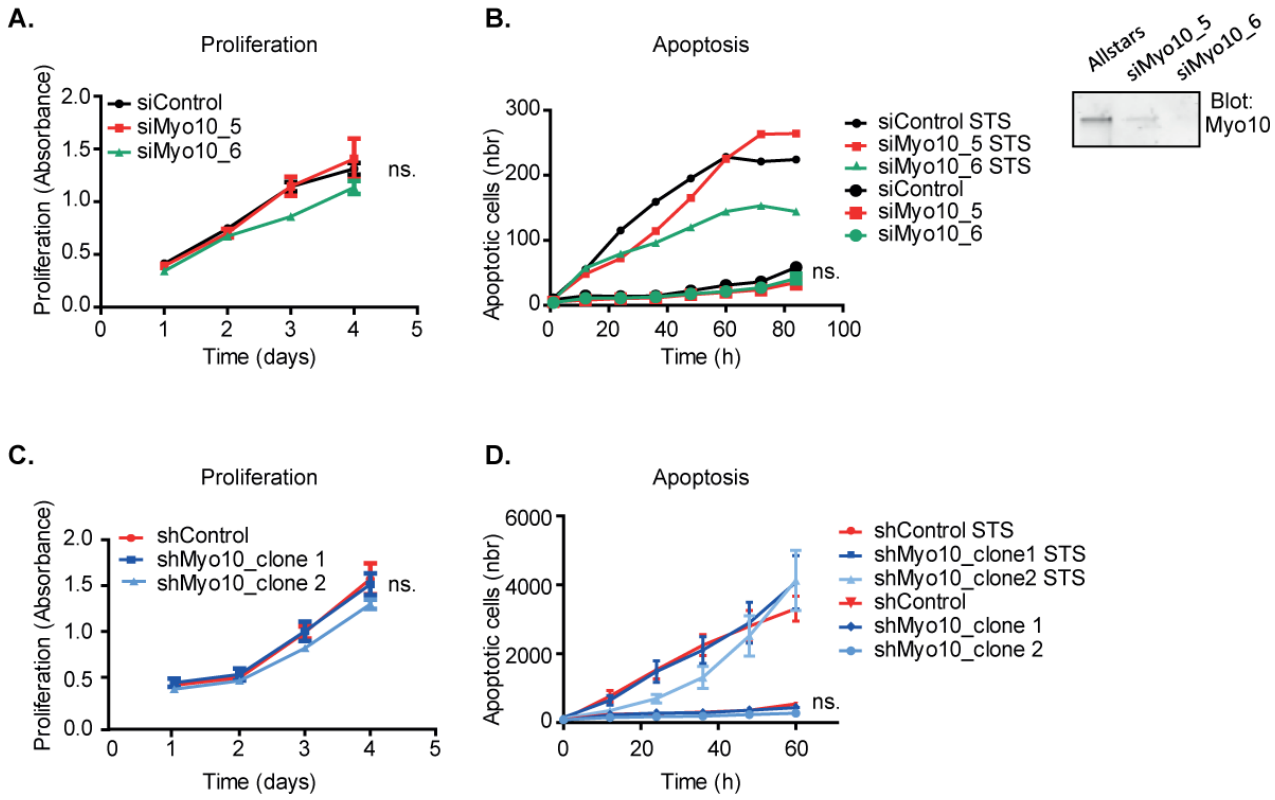

Figure S3

Silencing of Myo10 does not affect the proliferation or apoptosis of MDA-MB-231 cells in vitro. (**A and C**) Proliferation of control or siMyo10 (A) or shMyo10 (C) was measured by WST-1 staining every 24 h. Two individual Myo10 targeting oligos and two different shMyo10 clones were used. n (wells)=10 (**B and D**) Apoptosis of siMyo10 (B) and shMyo10 (D) cells was analyzed by measuring the Caspase 3/7 activity by CellPlayer 96-Well Kinetic Caspase-3/7 Apoptosis Assay Kit (Nucview). The number of apoptotic cells was analyzed by Incucyte ^{TM} FLR. n(images)=10. Staurosporine (STS, 10nM) was used as positive control.

Supplementary Figure 4

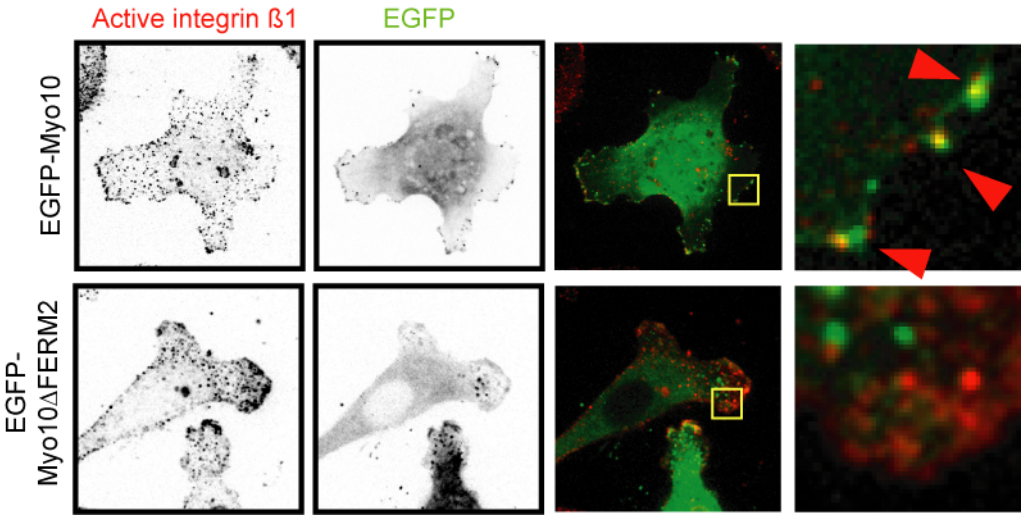

Figure S4

Myo10–mediated targeting of integrin to the filopodia tip.

MDA-MB-231 cells transfected with EGFP-Myo10 and EGFP-Myo10ΔFERM2 (green) were fixed and stained against active β1-integrin (9EG7, red). Cells were imaged with confocal microscope to visualize the localization of β1-integrin at the cell edge. Representative images are shown.

Supplementary Figure 5

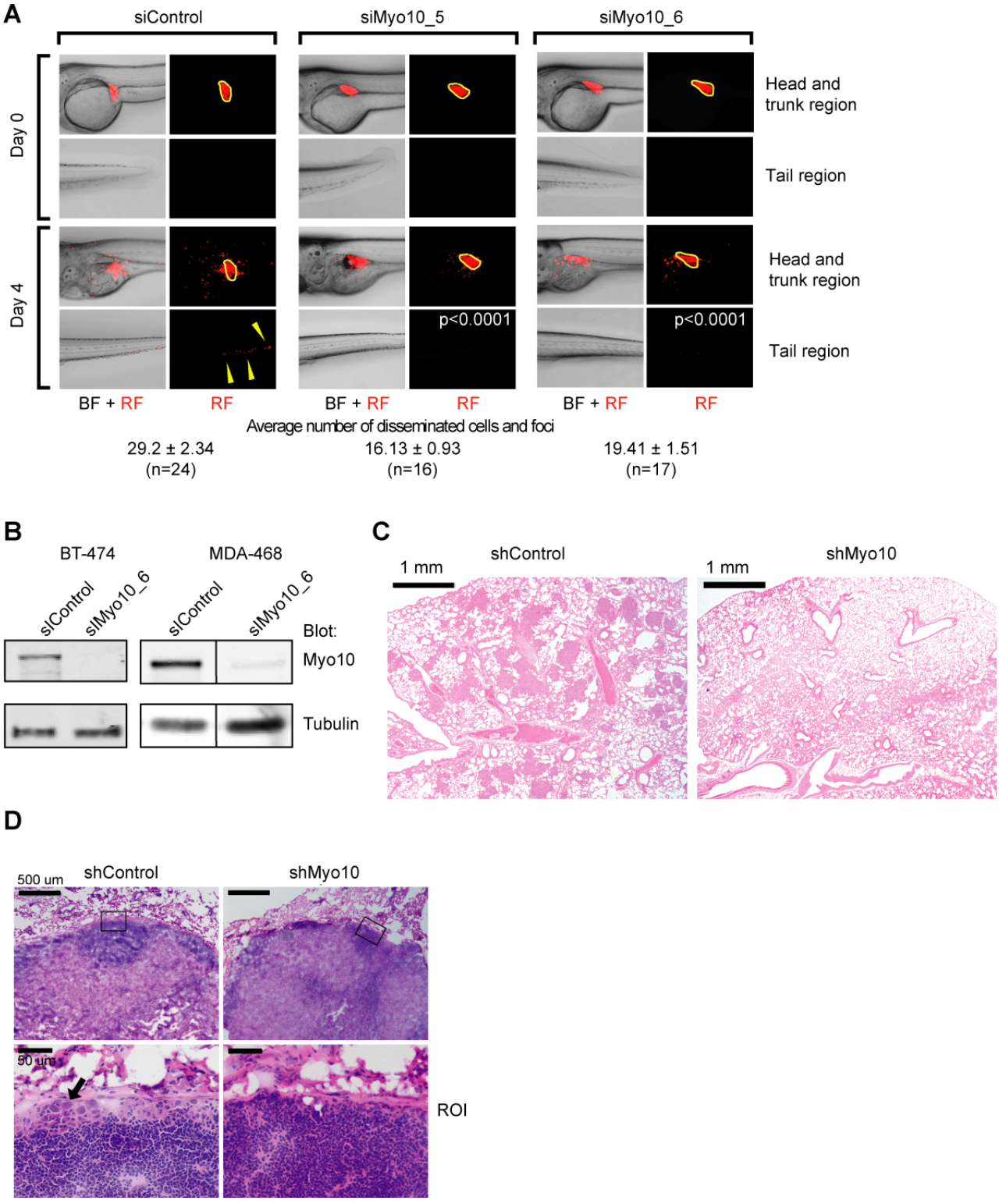

Figure S5

Silencing of Myo10 inhibits cancer cell dissemination in zebrafish embryos. (**A**) Dissemination and invasion of the tumor cells in zebrafish embryos. MDA-MB-231 cells transfected with control siRNA, Myo10 siRNA #5 or #6 were microinjected into zebrafish embryos 48 h postfertilization. Disseminated tumor cells and foci were observed 4 days postimplantation. Yellow circle indicates the originals place of microinjected cells. Yellow arrowheads indicate disseminated cells. Quantifications show the average number of disseminated

tumor cells and foci ($n > 20$ embryos/group). Mean±SEM and Mann-Whitney test are shown. (**B**) A western blot showing the silencing of Myo10 in BT-474 and MDA-468 cell lines after 48 h. Lanes were run on same gel but were noncontiguous in the case of MDA-468. (**C**) Low magnification images from H&E stained lungs from Figure 4D. Lung colonization of MDA-MB-231 cells into mouse lungs was studied in vivo by injecting control or Myo10 silenced cells into the tail vein of nude mice. Lung colonization was analyzed after 4 weeks from frozen sections by H&E staining. (**D**) An orthotopic metastasis assay was performed by injecting Myo10 or control shRNA–expressing MDA-MB-231 cells to mammary fat pads of nude mice. Systemic spreading of the cancer cells was assessed after 6 weeks from frozen contralateral lymph node tissue sections. Metastatic lesion is indicated with an arrow.

Supplementary Figure 6

A

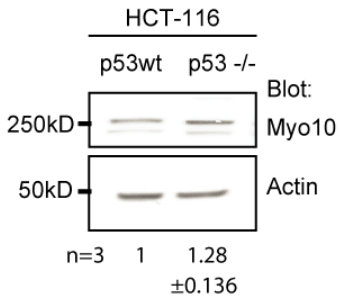

B

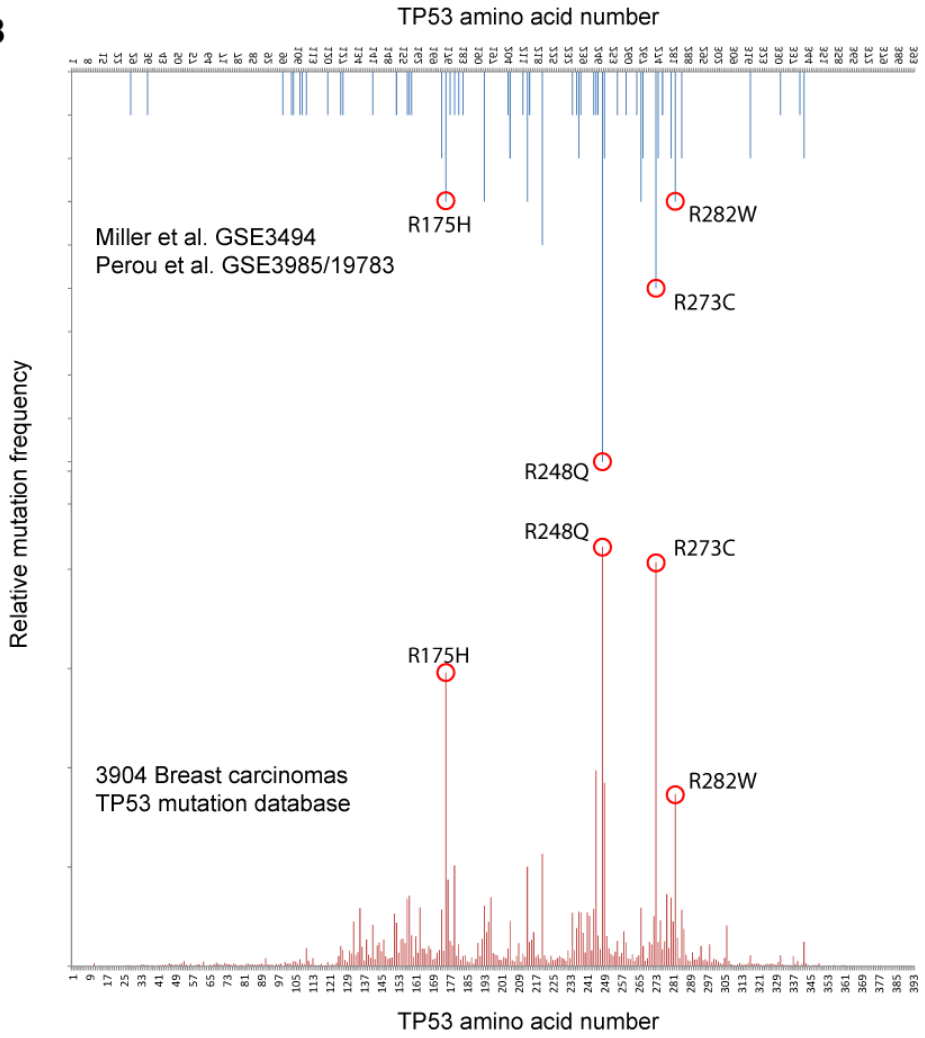

C

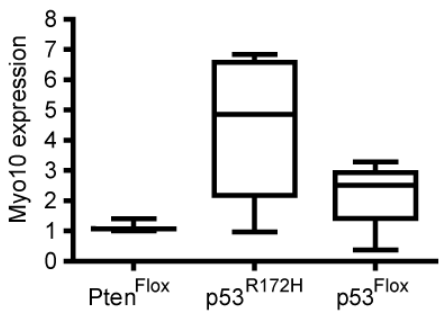

D

Probeset ID	Gene symbol	Step-up p-value	Fold change
1422544_at	Myo10	0.002	2.09
1450650_at	Myo10	0.044	1.57
1454731_at	Myo10	0.049	1.52

Figure S6

Mutant p53 regulates Myo10 levels. (**A**) Western blot of Myo10 in wild-type p53 or p53 null (-/-) HCT-116 cells. Tubulin is shown for loading control. The number of experiments (n) and the quantification of Myo10 levels relative to the control are shown. (**B**) The frequencies of different p53 mutations in Miller et al. (Miller et al. 2005) and Naume et al. (Naume et al. 2007) datasets compared to reference dataset (http://p53.fr/TP53_database_download/TP53_tumor_database/tumor_database.html), containing information of p53 mutations in 3409 breast carcinomas. (**C**) Myo10 expression was analysed from pancreatic ductal epithelial cells generated from the different transgenic mouse models through isolation from mouse pancreata and short term culture in tissue culture. The microarray data show that Myo10 expression is significantly higher in p53R172H tumors compared to the other subtypes analyzed (Ptenflox and P53flox). (**D**) The expression of Myo10 was determined by qRT-PCR from RNA isolated from pancreatic ductal adenocarcinoma (PDAC) mouse model tumor tissues. Four tumors were analyzed from each group..

Supplementary Figure 7

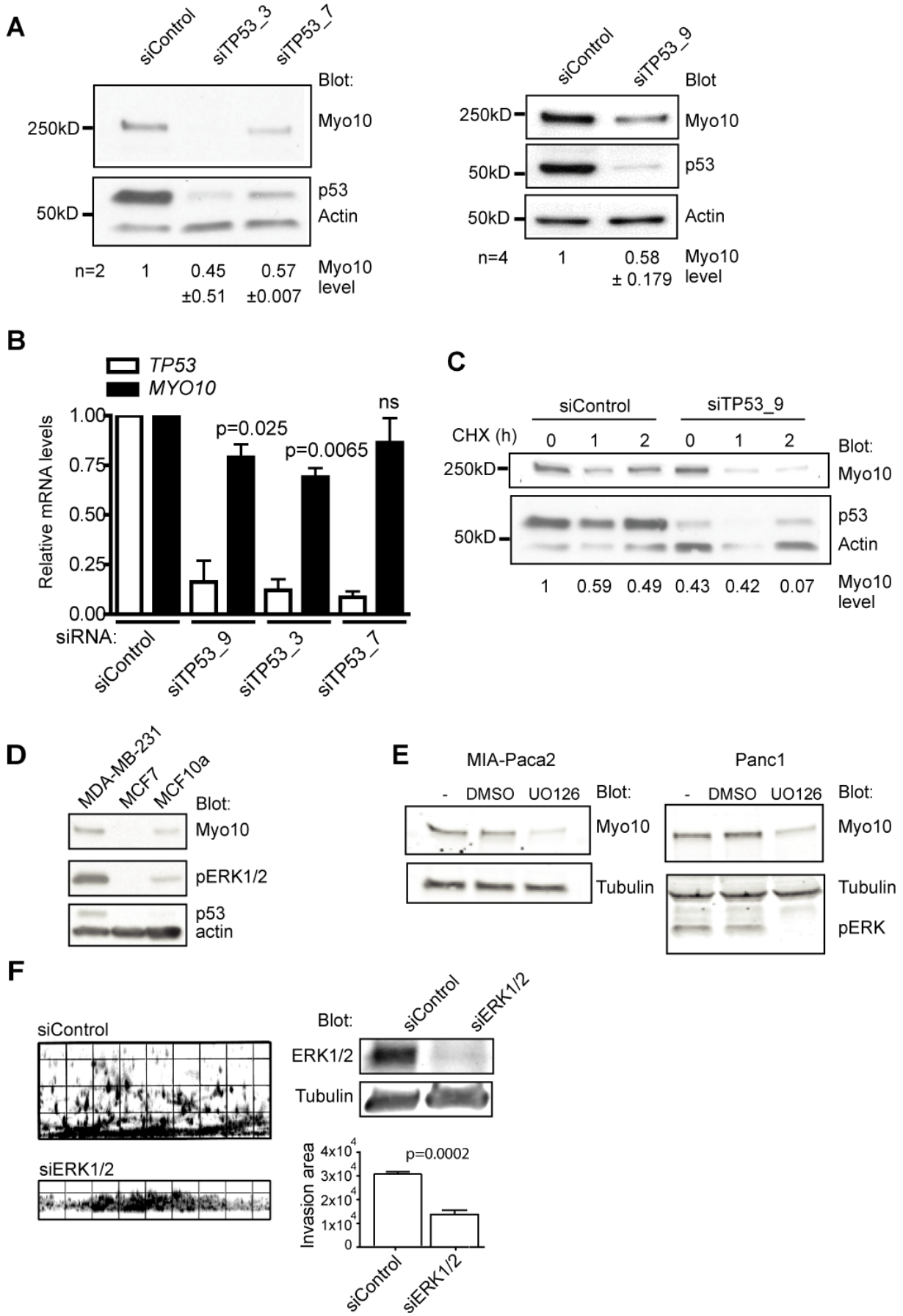

Figure S7

Mutant p53 regulates Myo10 levels and Myo10 expression is required for mutant p53–driven invasion. (**A**) Western blot of Myo10 in MDA-MB-231 cells after 72 h of siRNA silencing of mutant p53 with three p53-targeting oligos. Actin and p53 were blotted for silencing and loading controls. The number of experiments (*n*) and the quantification of Myo10 levels relative to the control are shown. (**B**) *MYO10* mRNA levels were analyzed in MDA-MB-231 cells 48 h after siTP53 (targeting mutant p53 in MDA-MB-231 cells) or siControl transfections using Taqman RT-qPCR. The Mean±SEM and Mann Whitney test p values are shown. *n*(siControl) = 7, *n*(sip53_9) = 5 and *n*(sip53_3 and sip53_7) = 2. (**C**) Mutant p53 silenced MDA-MB-231 cells were treated with 20 μM cycloheximide (CHX) for the indicated times. Cells lysates were analyzed by Western blotting using the indicated antibodies. Quantification of Myo10 levels relative to the loading control is shown. (**D**) A western blot showing the phosphorylated ERK1 and 2 (pERK1/2) levels in MDA-MB-231, MCF7 and MCF10a cells. (**E**) Western blot of Myo10 in MIA-Paca2 and Panc1 pancreatic cancer cell lines were treated over night with MEK inhibitor (UO126, 10 μM). DMSO was used as control. Tubulin was used as loading control and pERK antibody was used to validate MEK inhibition. (**F**) Invasion of siControl or siERK1 and ERK2 silenced phalloidin-488 stained MDA-MB-231 cells after 4 days of invasion. Images show side views of invasion and quantitation shows the average invasion area (A.U.) from two independent experiments.

Supplementary Figure 8

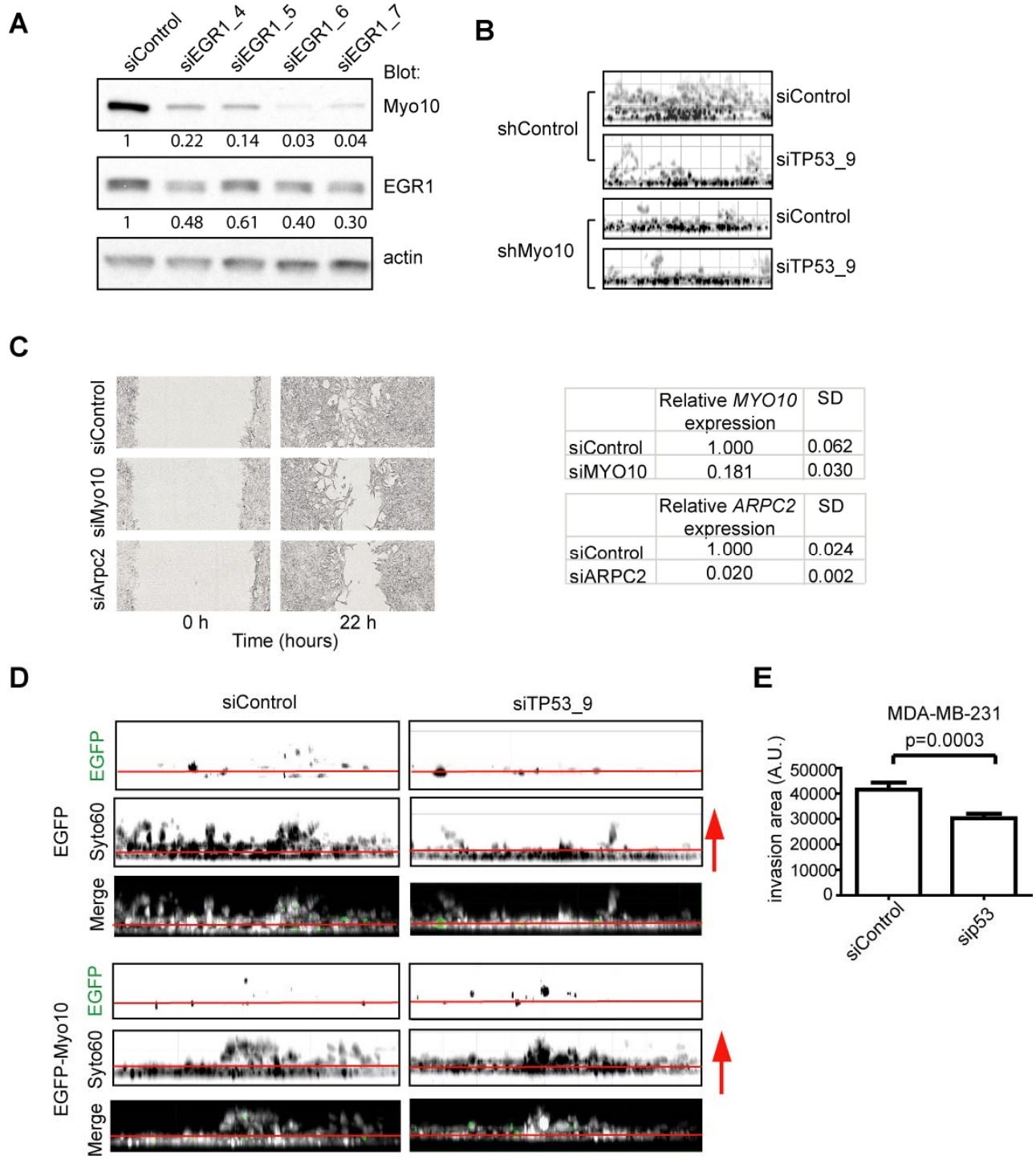

	Relative *MYO10* expression	SD
siControl	1.000	0.062
siMYO10	0.181	0.030

	Relative *ARPC2* expression	SD
siControl	1.000	0.024
siARPC2	0.020	0.002

Figure S8

Mutant p53 regulates cancer cell invasion by upregulating Myo10. (**A**) Western blot showing Myo10 expression upon silencing of EGR1 for 48 h with four different EGR1 targeting oligos. (**B**) Representative images of the MDA-MB-231 cell invasion assay shown in Figure 7E. Control and Myo10 shRNA silenced

MDA-MB-231 were transiently silenced with p53 siRNA for 48 h prior the invasion experiment. Images show side views of invasion after 4 days of invasion (**C**) Representative images of the PDAC invasion assay shown in Figure 7F. siRNA mediated Myo10 and ARPC2 silencing was quantified by qPCR. (**D**) Representative images of the invasion assay shown in Figure 7H. Matrigel invasion of pooled siControl or. Images show side views of Matrigel invasion of p53 silenced and Myo10-GFP transfected MDA-MB-231 cells after 3 days of invasion. The arrow indicates the direction of invasion. The noninvaded cells at the bottom of the wells are below the red line and the percentage of invaded GFP-positive cells from all GFP-positive cells was quantified by ImageJ. (**E**) Quantification of total invasion of MDA-MB-231 cells upon mutant p53 silencing from the experiment shown in Figure 7I. Invasion was analyzed by Syto60 staining and quantifying the invasion area using ImageJ.

Movie S1

Myo10–mediated targeting of integrin to the filopodia tip is critical for invasion. (**A**) U-87MG cells expressing EGFP-Myo10 (green) stained with fluorescently labeled β1-integrin antibody (red). Timelapse images of filopodia dynamics acquired at 10 second intervals, frame rate 7 fps. β1-integrin is mostly seen at the filopodia tip. Scale bar 5 μm.

Supplemental experimental procedures

Cell culture reagents

MDA-MB-231 human breast adenocarcinoma cells (American Type Culture Collection, ATCC) were maintained in Dulbecco's modified Eagle's medium (DMEM, 4500 mg/l glucose, Sigma) containing 1% nonessential amino acids (Sigma), 1% L-Glutamine (Gibco), and 10% fetal bovine serum (FBS). MCF10A cells (ATCC) were maintained in 1:1 DMEM (4500 mg/l glucose)-HAMs F12 (Gibco), 5% horse serum (Gibco), 1 % L-Glutamine, 10 µg/ml insulin, 5 µg/ml hydrocortisone (Sigma), 20 ng/ml hEGF (Peprotech, LTD), and 100 ng/ml choleratoxin. MCF7 were maintained in DMEM (1000mg/l glucose) supplemented with 10% FBS and 1% L-glutamine. Human colon carcinoma HCT116-p53 -/- were cultured in DMEM (4500 mg/l glucose) containing 10% FBS and 1% L-glutamine.

DNA constructs

To create stabile Myo10-silenced cell lines, MDA-MB-231 cells were transfected overnight with 2 µg of shMyo10 (sc-43241-SH, Santa Cruz) plasmid with Lipofectamine 2000 (Invitrogen) on a 6-well plate (Corning) according to the manufacturer's instructions, followed by selection with 1 µg/ml of puromycin dihydrochloride (Sigma) until the control cells were dead. After the selection, the puromycin concentration was reduced to 0.2 µg/ml. Fluorescence-assorted cell sorting was used to create one-cell clones, in which Myo10 was efficiently silenced. Cloning of EGFP-Myo10 and EGFP-Myo10ΔFERM2 constructs have been described in (Zhang et al. 2004) and the constructs were a kind gift from Dr. S. Strömblad, Karolinska Institutet, Huddinge). The p53-R273H construct was cloned as described in (Bullock et al. 1997). shp53 pSUPERretro-puro as well as RNAi-resistant R175H (hp53 R175H in pRRLsin.PPTs.hCMV.GFPpre) and wtp53 (mp53ASwt pBABE-puro) constructs are described in Adorno et al. (Adorno et al. 2009) and the constructs were a kind gift from Dr. S. Piccolo, University of Padova, Italy). Transfections were done using Lipofectamine 2000 (Invitrogen) according to the manufacturer's instructions.

siRNA transfections

TP53 was silenced by 80 nM of siRNA for 48 hours (Qiagen: Hs_TP53_9 Hs_TP53_3 and Hs_TP53_7), and MYO10 was silenced by 100 nM for 48 hours (Qiagen: Hs_MYO10_5 and Hs_MYO10_6) using a Hiperfect transfection reagent according to the manufacturer's instructions. EGR-1 was silenced using by 80 nM of siRNA for 48 hours (Qiagen Flexitube Hs_EGR1_4, Hs_EGR5, Hs_EGR6_Hs_EGR7 (20 nM of each). MAP-kinases ERK1 and ERK2 were silenced with following siRNAs: ON-TARGETplus Smart pool Human MAPK3 (ERK1) siRNA (LU-

003592-00-0002: Dharmagon) and MAPK1 ON-TARGETplus Smart Pool MAPK1 (ERK2) siRNA (LU-003555-00-0002, Dharmagon). Allstars negative control siRNA (Qiagen) was used as a control siRNA (siControl) for all experiments.

Quantitative real-time polymerase chain reaction

Total RNA was extracted by an RNAeasy Mini Kit (Qiagen) and converted to cDNA using a high-capacity cDNA reverse transcription kit (Applied Biosystems) according to the manufacturer's instructions. Expression of MYO10 and TP53 and EGR1 was measured by TaqMan® probe–based quantitative real-time polymerase chain reaction using the Real-Time PCR HT7900 (Applied Biosystems). Glyceraldehyde 3-phosphate dehydrogenase (GAPDH) was used as endogenous control. The following primers were ordered from Sigma: MYO10_forward AGGACTTTCCACCTGATTGC, MYO10_reverse CGTGGACCTGACCTAGCA (TaqMan® probe #20, Roche), TP53_forvard TCCTCCATGGCAGTGACC, TP53_reverse CTTTCCACGACGGTGACA (TaqMan® probe #71, Roche), GAPDH_reverse GCCCAATACGACCAAATCC, and GAPDH_forward AGCCACATCGCTCAGACA (TaqMan® probe #60, Roche). EGR-1_forward AGCCCTACGAGCACCTGAC, EGR-1_reverse GGTTTGGCTGGGGTAACTG (TaqMan® probe #22, Roche) For Mouse samples, Quantative RT-PCR was carried out using DyNAmo SYBR Green 2-step qRT-PCR Kit (Thermo Scientific). Reactions were run using a DNA-engine system (Bio-Rad) and Opticon Monitor3 analysis software (MJ Research). Primers for Myo10 were TGACAACCAATGTGTCCTCATC (forward) and AGGCCCAGGTCCAAAGTCT (reverse) and were used at a concentration of 0.5 μM. Relative quantitation of Myo10 was calculated using the $\Delta\Delta C$t method using β-actin for normalisation.

Immunohistochemical stainings

For immunohistochemistry, 5 μm tissue sections were cut onto SuperfrostTM + slides, deparaffinized with xylene, and rehydrated in a graded alcohol series. Endogenous peroxidase activity in the tissue was blocked with 1% hydrogen peroxide, and antigen retrieval was carried out in sodium citrate (0.01 mol/l, pH 6.0) using an autoclave (at 120° C for 2 minutes). Myo10 expression was detected using a rabbit polyclonal antibody (cat#22430002, Novus Biologicals, Cambridge, UK; dilution 1:2000). The primary antibody was diluted in a PowerVision pre-antibody blocking solution and incubated overnight at 4° C, and binding of the primary antibody was detected using a PowerVision + Poly-Horseradish Peroxidase histostaining kit (DPVB + 110DAB; Immunovision Technologies Co., Daly City, CA, USA) following the manufacturer's instructions. Expression of Myo10 was graded as negative (-) or weakly (+), moderately (++), or strongly (+++) positive, when at least 10% of the tumor cells showed immunostaining.

Immunohistochemical stainings for frozen sections

Tissues were embedded in Tissue-Tek® O.C.T.™ Compound (Sakura). Sections were acetone fixed for 10 min at -20 ^{0}C. Permeabilization was done with 0.3% Triton-X in 2% BSA followed by 30 min blocking in 30 % Horse serum-PBS and staining with 1:400 α-vimentin (HPA001762, Sigma), 1 h staining in RT followed by washes with PBS and 1 h incubation with 1:400 Alexa Fluor ® α-rabbit-555 (Life technologies) and Dapi (0.1 ug/ml).

In silico data analysis

The breast cancer raw datasets (GSE3494 (Miller et al. 2005) and GSE3985/GSE19783 (Naume et al. 2007) were downloaded for the public source GEO gene expression omnibus data repository (Edgar et al. 2002). Addition annotation was retrieved from the corresponding publications and supplementary data. Data analysis software based on the R (Ihaka 1998) and Bioconductor (Gentleman et al. 2004) was written. An affymetrix gene expression microarray (Miller et al. 2005) was normalized by the RMA method utilizing the affy R package (Irizarry et al. 2003) and custom CDF (Dai et al. 2005) to link all oligonucleotides to their corresponding ensemble gene IDs. Agilent gene expression microarrays (Naume et al. 2007) were normalized utilizing the limma R package (Smyth and Speed 2003) and the biomaRt R package (Durinck et al. 2005) to link all bead probes to their corresponding ensemble gene IDs. Data were log2 transformed and median centered in a genewise manner. The Kaplan-Meier plot implementation is based on the survival R package (T.M. Therneau 2006). The distribution and box plot implementation is based on the R base distribution.

Western blotting

Following antibodies were used in 1:1000 dilutions: Anti-Myo10 (845-944, Strategic Diagnostics, Inc.), anti-Talin (T3287, Sigma), anti-beta-actin (A1978, Sigma), anti-integrin β1 (BD Transduction Laboratories), anti-alpha-tubulin (12G10, Hybridoma Bank), and anti-p53 (DO-7, Santa Cruz), HSC70/hsp73 (ADI-SPA-815-F, ENZO Life science), pERK1/2 (Thr 202/Tyr 204, #9102, Cell Signaling Technology), anti-EGR-1 (sc-110, Santa Cruz Biotechnology), ERK1/2 (L34F12) p44/42 (#4696, Cell signalling Technology).

*Flow cytometry analysis of lung colonization assay*Lung cells were isolated as described in Vuoriluoto et al. (Vuoriluoto et al. 2011). Shortly, lungs were cut into pieces and incubated in 50 μg/ml of collagenase XI (C7657, Sigma) for 1.5 h at37°C on rotation. Cells were passed through the 70 μm strainers (BD Falcon) in order to obtain single cell suspension. Cells were fixed with 4% PFAH for 10 minutes. Half of the cell suspension was permeabilized with 0.3 % Triton-X in PBS and stained with 1:100 anti-vimentin (sc-6260, Santa Cruz) and 1:400 Alexa Fluor ® α-mouse-647.

The other half was stained with 1:100 anti-HLA (Hb116, Koskinen et al. 2004) and 1:400 Alexa Fluor ® α-mouse-647.

Cell migration, adhesion and spreading assays

Time-lapse microscopy was used to follow the migration of siRNA- and shRNA-mediated silencing of Myo10. Cells were embedded in 10% growth factor–reduced Matrigel matrix (BD Biosciences) in full growth medium, allowed to spread for few hours, and then imaged for 22 hours with 15 minute intervals. ImageJ plugin MTrackJ (Meijering et al. 2012) was used for the tracking of migrating cells. Mean square displacement for the tracks was measured using the x and y coordinates of the tracks. For cell adhesion, a 96-well plate was coated with 100 µl of 5 µg/ml of fibronectin (Merck) overnight at +4° C. MDA-MB-231 cells were suspended in serum-free media (in 800 cells/ml). Coated wells were blocked with 0.1% BSA in PBS for 1 hour at +37°C. 100 µl of cell suspension was added to each well, and adhesion of the cells was analyzed at 30 minute and 60 minute time points. Nonadhered cells were removed by washing with PBS, and bound cells were treated with 4% PFA for 10 minutes at room temperature (RT). Adhered cells were stained with 100 µl of 20 µg/ml of propidium iodide for 30 minutes, and the cell amount was analyzed by fluorescent plate reader. The morphology of cells during the spreading was analyzed at 60 minute timepoint. Adherent cells were treated with 4% PFA for 10 minutes and stained for phalloidin, as previously described.

Zebrafish invasion assay

Fertilized zebrafish eggs were collected and kept in embryo water (E3) containing 0.2 mM 1-phenyl-2-thio-urea (PTU) at 28°C under laboratory standard conditions. At 48 hours post fertilizations, zebrafish embryos were dechorionated with help of two sharp tip forceps and then anaesthetized in a 0.04 mg/ml of tricaine (Ethyl 3-aminobenzoate methanesulfonic acid salt, Sigma-Aldrich) solution. Anaesthetized embryos were subsequently placed on top of a modified agarose gel. Tumor cells were labeled with 2 µg/ml of 1,1´-Dioctadecyl-3,3,3´,3´-tetramethylindocarbocyanine perchlorate (red fluorescent dye) prior to implantation. Tumor cells were counted and resuspended in 1% serum containing medium (DMEM, Sigma, Germany). A volume of approximately 5 nl containing 100-500 cells were injected into each embryo with help of Non-filamentous borosilicate glass capillary needles (1.0 mm in diameter, World Presicion Instruments, Inc. USA) connected to a Manipulator (MN-151, Narishige, Japan) and an Eppendorf microinjector (FemtoJet 5247, Eppendorf, Germany). Cells were implanted into the perivitelline space of the embryo and implanted embryos were immediately transferred into the embryo water

containing PTU and were kept under the same standard condition as mentioned above. Tumor cell spreading was investigated 4 days post injection using fluorescent microscope (Nikon, Japan).

Chromatin immunoprecipitation

Protein-chromatin complexes were cross-linked with 0.37 % formaldehyde for 10 minutes followed by quenching with 0,125 M glysine. Cells were lysed in 500 µl of lysis buffer [0.01 M Tris-HCl,(pH 8), 0.01 M NaCl, 0.2 % Nonidet P-40 and 500 µM phenylmethanesulfonylfluoride (PMSF)] and incubating for 10 min. Chromatin was sheared by sonication in 1 ml of Radio-immunoprecipitation assay-buffer (RIPA) (1% NP-40, 0.5% Na deoxycholate, 0.1 % SDS, 50 mM This-HCl (pH8.4), 150 mM NaCl) using water bath sonicator (Bioruptor, Cosmo Bio Co LTD). Pre-clearing was performed by adding 75 µl of protein G-sepharose beads (GE Healthcare) and incubating for 1 hour at 4 ºC on rotation. Chromatin from 6-10 million cells was used for each immunoprecipitation. Immunoprecipitations were performed by adding10 µg of antibody (Rabbit IgG (Santa Cruz Biotechnology), H3K4me3 (ab8580, Abcam), EGR-1 (sc-110, Santa Cruz Biotechnology)) and incubating overnight at +4 ºC on a rotation. Immunocomplexes were collected by 2 h incubation with100 µl of G-sepharose beads, followed by washes with four times 500 µl of RIPA-buffer, once with IP-wash buffer (0.01 M Tris-HCl (pH 8), 0.25 M LiCl, 0.001 M EDTA, 1% Nonodet P-40) and once with TE-buffer (0.01 M Tris, 0.001 M EDTA, pH 8.0). Immunoprecipitates were eluted from the beads by 15 min incubation in freshly prepared IP-elution buffer (100mM NaHCO3 + 1% SDS). DNA was purified by 25:24:1 phenol-chlorophorm-isoamyl (pH 7.8) extraction. ChIP was analyzed by PCR using *MYO10* specific primers (Forward: AAGGTGCGTTTCCGTTTGCG, Reverse: TATTGGGCTTCCTGCACC)

Primers were designed based University of California Santa Cruz (UCSC) genome browser (http://genome.ucsc.edu/) database prediction.

References:

Adorno, M., M. Cordenonsi, M. Montagner, S. Dupont, C. Wong, B. Hann, A. Solari, S. Bobisse, M. B. Rondina, V. Guzzardo, A. R. Parenti, A. Rosato, S. Bicciato, A. Balmain and S. Piccolo (2009). "A Mutant-p53/Smad complex opposes p63 to empower TGFbeta-induced metastasis." Cell **137**(1): 87-98.

Bullock, A. N., J. Henckel, B. S. DeDecker, C. M. Johnson, P. V. Nikolova, M. R. Proctor, D. P. Lane and A. R. Fersht (1997). "Thermodynamic stability of wild-type and mutant p53 core domain." Proc Natl Acad Sci U S A **94**(26): 14338-14342.

Dai, M. H., P. L. Wang, A. D. Boyd, G. Kostov, B. Athey, E. G. Jones, W. E. Bunney, R. M. Myers, T. P. Speed, H. Akil, S. J. Watson and F. Meng (2005). "Evolving gene/transcript definitions significantly alter the interpretation of GeneChip data." Nucleic Acids Research **33**(20).

Durinck, S., Y. Moreau, A. Kasprzyk, S. Davis, B. De Moor, A. Brazma and W. Huber (2005). "BioMart and Bioconductor: a powerful link between biological databases and microarray data analysis." Bioinformatics **21**(16): 3439-3440.

Edgar, R., M. Domrachev and A. E. Lash (2002). "Gene Expression Omnibus: NCBI gene expression and hybridization array data repository." Nucleic Acids Res **30**(1): 207-210.

Gentleman, R. C., V. J. Carey, D. M. Bates, B. Bolstad, M. Dettling, S. Dudoit, B. Ellis, L. Gautier, Y. C. Ge, J. Gentry, K. Hornik, T. Hothorn, W. Huber, S. Iacus, R. Irizarry, F. Leisch, C. Li, M. Maechler, A. J. Rossini, G. Sawitzki, C. Smith, G. Smyth, L. Tierney, J. Y. H. Yang and J. H. Zhang (2004). "Bioconductor: open software development for computational biology and bioinformatics." Genome Biology **5**(10).

Ihaka, R. (1998). "R: Past and future history." Dimension Reduction, Computational Complexity and Information **30**: 392-396.

Irizarry, R. A., B. Hobbs, F. Collin, Y. D. Beazer-Barclay, K. J. Antonellis, U. Scherf and T. P. Speed (2003). "Exploration, normalization, and summaries of high density oligonucleotide array probe level data." Biostatistics **4**(2): 249-264.

Meijering, E., O. Dzyubachyk and I. Smal (2012). "Methods for cell and particle tracking." Methods Enzymol **504**: 183-200.

Miller, L. D., J. Smeds, J. George, V. B. Vega, L. Vergara, A. Ploner, Y. Pawitan, P. Hall, S. Klaar, E. T. Liu and J. Bergh (2005). "An expression signature for p53 status in human breast cancer predicts mutation status, transcriptional effects, and patient survival." Proc Natl Acad Sci U S A **102**(38): 13550-13555.

Naume, B., X. Zhao, M. Synnestvedt, E. Borgen, H. G. Russnes, O. C. Lingjaerde, M. Stromberg, G. Wiedswang, G. Kvalheim, R. Karesen, J. M. Nesland, A. L. Borresen-Dale and T. Sorlie (2007). "Presence of bone marrow micrometastasis is associated with different recurrence risk within molecular subtypes of breast cancer." Mol Oncol **1**(2): 160-171.

Smyth, G. K. and T. Speed (2003). "Normalization of cDNA microarray data." Methods **31**(4): 265-273.

T.M. Therneau, B. A. (2006). "The rpart package." Archive Network http://cran.stat.ucla.edu (2006).

Vuoriluoto, K., H. Haugen, S. Kiviluoto, J. P. Mpindi, J. Nevo, C. Gjerdrum, C. Tiron, J. B. Lorens and J. Ivaska (2011). "Vimentin regulates EMT induction by Slug and oncogenic H-Ras and migration by governing Axl expression in breast cancer." Oncogene **30**(12): 1436-1448.

Zhang, H., J. S. Berg, Z. Li, Y. Wang, P. Lang, A. D. Sousa, A. Bhaskar, R. E. Cheney and S. Stromblad (2004). "Myosin-X provides a motor-based link between integrins and the cytoskeleton." Nat Cell Biol **6**(6): 523-531.